DOI: 10.1002/chem.200700011

Synthesis, Characterization, and Electrochemiluminescence of Luminol-Reduced Gold Nanoparticles and Their Application in a Hydrogen Peroxide Sensor

Hua Cui,* Wei Wang, Chun-Feng Duan, Yong-Ping Dong, and Ji-Zhao Guo[a]

Abstract: It was found that chloroauric acid ($HAuCl_4$) could be directly reduced by the luminescent reagent luminol in aqueous solution to form gold nanoparticles (AuNPs), the size of which depended on the amount of luminol. The morphology and surface state of as-prepared AuNPs were characterized by transmission electron microscopy, UV/visible spectroscopy, X-ray photoelectron spectroscopy, FTIR spectroscopy, and thermogravimetric analysis. All results indicated that residual luminol and its oxidation product 3-aminophthalate coexisted on the surface of AuNPs through the weak covalent interaction between gold and nitrogen atoms in their amino groups. Subsequently, a luminol-capped AuNP-modified electrode was fabricated by the immobilization of AuNPs on a gold electrode by virtue of cysteine molecules and then immersion in a luminol solution. The modified electrode was characterized by cyclic voltammetry, electrochemical impedance spectroscopy, and scanning electron microscopy. The as-prepared modified electrode exhibited an electrochemiluminescence (ECL) response in alkaline aqueous solution under a double-step potential. H_2O_2 was found to enhance the ECL. On this basis, an ECL sensor for the detection of H_2O_2 was developed. The method is simple, fast, and reagent free. It is applicable to the determination of H_2O_2 in the range of 3×10^{-7}–1×10^{-3} mol L^{-1} with a detection limit of 1×10^{-7} mol L^{-1} ($S/N=3$).

Keywords: gold · hydrogen peroxide · luminescence · nanoparticles · sensors

Introduction

Electrochemiluminescence (ECL) is a valuable analytical tool which has been widely used in immunoassays, clinical diagnosis, and trace detection due to its high sensitivity, low background, wide dynamic range, and simple formats.[1–5] The immobilization of ECL reagents on solid supports has been an important subject for developing sensors, microchips, and portable detectors.[2,6–8] In the past, much attention has been paid to the immobilization of tris(2,2′-bipyridyl)ruthenium(II) (TBR) and its derivatives, one of the most commonly used ECL reagents, because the organic bipyridyl group and the positive charge were helpful for the structural modification and immobilization and the ECL reagents are regenerable in ECL reactions.[7–11] To date, a series of methods has been proposed to immobilize TBR and its derivatives on various electrode materials for the detection of compounds, such as tripropylamine,[7–10] oxalate,[6,9] and ethanol.[11] However, the immobilization of TBR in such sensors based on ion exchange and/or electrostatic adsorption was greatly restricted by the instability.[1] Besides, only limited species can be detected by TBR-based ECL methods. Therefore, some effort should also be made towards the immobilization of other ECL reagents, such as luminol.

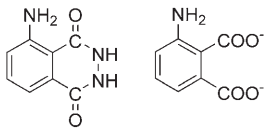

luminol AP^{2-}

Luminol is a popular ECL reagent with a rather high light efficiency. It has been widely used for the detection of various analytes.[1–3] However, the applications of luminol ECL in sensors have been limited, partially because it is a challenging subject to immobilize luminol on an electrode without decreasing its ECL activity. Until now, there have been only a few reports on luminol-based ECL sensors. Ouyang and Wang[12] developed an ECL sensor for the determination of glucose by immobilizing both luminol and glucose oxidase on a clay-modified electrode, through a covalent bond linked with the amino group of luminol. Recently, luminol-doped SiO_2 nanoparticles

[a] Prof. H. Cui, Dr. W. Wang, C.-F. Duan, Y.-P. Dong, J.-Z. Guo
Department of Chemistry
University of Science and Technology of China
Hefei, Anhui 230026 (P.R. China)
Fax: (+86) 551-360-0730
E-mail: hcui@ustc.edu.cn

were immobilized on the surface of the electrode, and an ECL sensor was developed for the determination of pyrogallol based on its enhancement of luminol ECL.[13] In another work, luminol-doped SiO_2 nanoparticles were linked to probe single-stranded DNA (ssDNA) as an ECL label to determine target ssDNA immobilized on the electrode.[14]

Gold nanoparticles (AuNPs) have been widely used in biosensors due to their excellent biocompatibility and ease of self-assembly through the Au–S bond.[15,16] It has been reported that a lot of amine compounds, including aliphatic amines,[17–19] aromatic amines,[18] and several amino acids,[20,21] could reduce $HAuCl_4$ to produce and stabilize gold colloids as protecting agents in both aqueous and organic solutions. The interaction linking AuNPs and amine molecules was attributed to the weak covalent interaction between gold and nitrogen atoms[22,23] and the electrostatic interaction between negatively charged AuNPs and positively charged amines in some cases.[19] As luminol is a type of reductive compound with an aromatic amine group and earlier work demonstrated that luminol could directly reduce $HAuCl_4$ in a reverse micelle solution to give rise to chemiluminescence[24] it was reasonable to deduce that luminol might reduce $HAuCl_4$ to produce AuNPs. This gives us an opportunity to immobilize luminol molecules on the surface of AuNPs, and then the resulting luminol-reduced AuNPs might be further linked to the electrode by virtue of bridging molecules which have affinity to both AuNPs and various electrode materials, as described in our previous work.[25]

Herein, we show that AuNPs can indeed be synthesized by the reduction of $HAuCl_4$ by luminol. The morphology and surface state of the resulting AuNPs were characterized by transmission electron microscopy (TEM), UV/visible spectroscopy, X-ray photoelectron spectroscopy (XPS), FTIR spectroscopy, and thermogravimetric analysis (TGA). The results showed that luminol and its oxidation product 3-aminophthalate (AP^{2-}) were capped on the surface of AuNPs as stabilizers. Moreover, the luminol-capped AuNPs were immobilized on the surface of a gold electrode by virtue of cysteine. The modified electrode was characterized by cyclic voltammetry (CV), electrochemical impedance spectroscopy (EIS), and scanning electron microscopy (SEM). The ECL of luminol capped on the surface of the electrode was studied by use of a double-step potential. It was found that luminol ECL could be generated by this electrochemical method and H_2O_2 could enhance the ECL. On this basis, an ECL sensor for the detection of H_2O_2 was developed. Hydrogen peroxide is a product of many enzymatic reactions.[26–28] The proposed sensor may be of great potential for the detection of biologically important compounds.

Results and Discussion

Synthesis and characterization of gold colloids: When $HAuCl_4$ solution was mixed with luminol solution, a wine-red- or purple-colored solution, depending on the amount of luminol, was formed, implying that $HAuCl_4$ might be reduced by luminol to AuNPs. Figure 1 and Figure 2A–E show

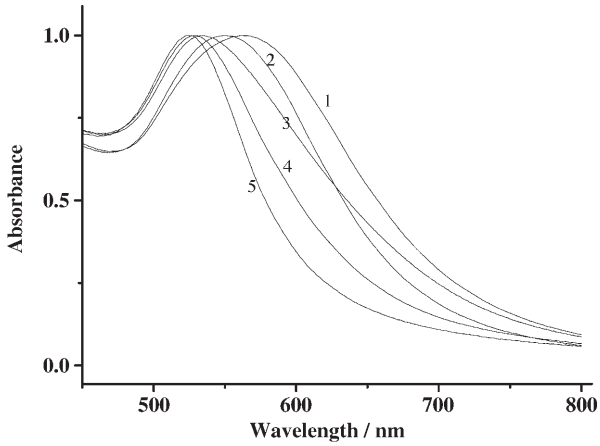

Figure 1. UV/Vis absorption spectra of AuNPs synthesized with varying amounts of luminol solution: $HAuCl_4$ solution (0.1‰, w/w; 100 mL) was mixed with 1.45 (curve 1), 1.50 (curve 2), 1.55 (curve 3), 1.60 (curve 4) and 1.80 mL (curve 5) luminol solution (0.01 mol L^{-1}). The maximum absorption wavelength λ and corresponding mean diameter D calculated from Figure 2A–E are 1: $\lambda = 561.5$ nm, $D = 35$ nm; 2: $\lambda = 550.5$ nm, $D = 29$ nm; 3: $\lambda = 534.5$ nm, $D = 25$ nm; ; 4: $\lambda = 530.0$ nm, $D = 20$ nm; 5: $\lambda = 523.5$ nm, $D = 14$ nm.

the UV/visible spectra (all the spectra were normalized at their surface plasmon absorption maximum for comparison) and TEM images, respectively, of the resulting solutions with different amounts of luminol, confirming the formation of AuNPs with different diameters. Moreover, it was also demonstrated that both the diameter of the nanoparticles and the maximum absorption wavelength increased with decreasing amounts of reductant luminol. The dependence of the size of the nanoparticles on the reductant luminol is consistent with that found in the citrate reduction method.[29]

The stability of the as-prepared colloid was found to be strongly dependent on the pH. When stored at 4 °C, the colloids were stable for at least six months without any visible precipitates if the pH was ≥ 8, whereas coagulation and precipitation occurred rapidly if the pH was < 3. Furthermore, the dried precipitates were easily redispersed in alkaline aqueous solutions, such as Na_2CO_3 and NaOH solutions. This observation implied that the surface of the AuNPs was negatively charged and the electrostatic repulsion was the main factor for the stabilization. At low pH values, most of the negatively charged groups were protonated, and consequently the coulombic repulsive interaction became weak and aggregation and precipitation occurred. This pH-dependent stability was very similar to earlier reports on carboxylic-protected AuNPs.[30,31] Moreover, the concentration of electrolyte in the colloids was another important factor for the stabilization. The addition of suitable amounts of salt could also lead to a rapid and efficient precipitation of AuNPs even in alkaline solution, which was utilized in the

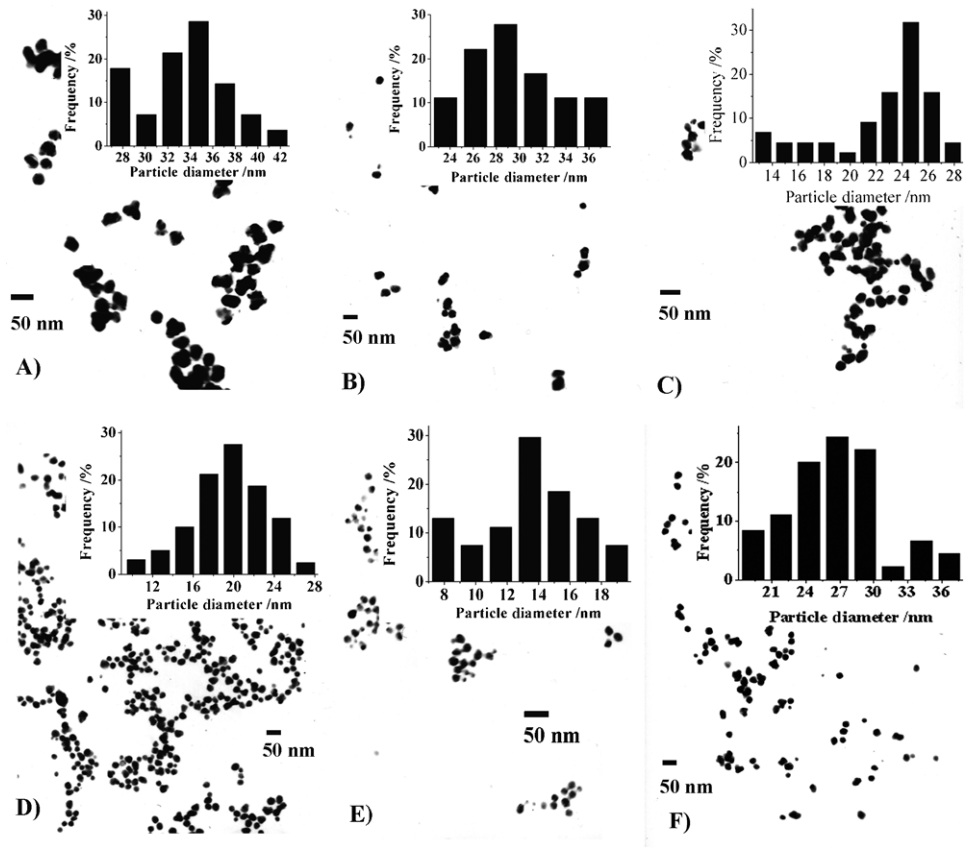

Figure 2. TEM images and the corresponding size distributions of AuNPs synthesized with varying amounts of luminol solution: A) 1.45, B) 1.50, C) 1.55, D) 1.60, and E) 1.80 mL. F) TEM image and size distribution of nanoparticles after a salt-out, centrifugation, and redispersion procedure to AuNPs in image (C).

salting-out process described in the Experimental Section. A high content of cations was reported to cause cross-linking with the negatively charged nanoparticles and the aggregation of these nanoparticles.[32,33] The amount of salt necessary for complete precipitation was also dependent on the pH. In a general range from pH 6 to 13, colloids at a higher pH needed more salt to achieve complete precipitation. The aggregation and precipitation caused by both acid (for pH) and salt (for electrolyte concentration) were accompanied by an observable color change of the colloids, which was a reflection of the aggregation of the nanoparticles.

Clarification of surface state of AuNPs: It has been reported that luminol could be oxidized by $HAuCl_4$ to the excited-state AP^{2-} in a reverse micelle solution, giving rise to light emission.[24] In the reaction, the final oxidation product of luminol was the ground state AP^{2-}. In our work, $HAuCl_4$ was reduced by luminol to form AuNPs and it was deduced that luminol was oxidized to AP^{2-}. Considering that both luminol and AP^{2-} contained the aromatic amino group in their molecular structures, it was reasonable to assume that luminol and AP^{2-} were coadsorbed onto the surface of AuNPs through the weak covalent interaction between gold and nitrogen atoms, according to the earlier reports on the interaction between amine compounds and AuNPs.[19,22,23] Therefore, both residual luminol and AP^{2-} were believed to coexist on the surface of AuNPs. UV/visible spectroscopy, XPS, TGA, and FTIR spectroscopy were used to obtain experimental evidence to support this coadsorption model. Colloids of particle diameter 25 nm were selected in all the following characterizations.

UV/visible spectroscopy: A 24 hour dialysis procedure (see below for details) was carried out to remove free luminol and AP^{2-} molecules from the colloids, so that true information about the surface of the AuNPs could be obtained by instrumental characterization. After dialysis, it can be seen that the luminol dual absorption peaks around 300 and 360 nm have almost disappeared in the UV/Vis spectrum of the dialyzed colloids (Figure 3, curve b) compared with that of the original colloids (curve a), and the maximal surface plasmon absorption wavelength remained at 534.5 nm but the intensity of the peak decreased. The decrease in absorption peak intensity was attributed to the di-

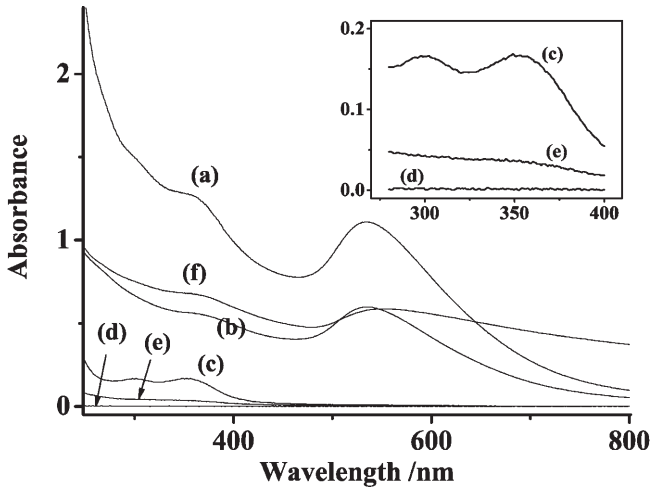

Figure 3. UV/Vis absorption spectra of 25 nm AuNPs before and after dialysis and salt-out procedures. a) Original 25 nm gold colloids, b) dialyzed colloids, c,d) dialyzed-out solution for the first and last dialysis procedures, respectively, e) supernatant after salt-out of dialyzed colloids, and f) redispersed colloids of AuNPs precipitated during the salt-out process. Inset: magnification of curves c–e in the range of 280–400 nm.

lution effect during the dialysis procedure. On the contrary, the dual peak of luminol could be detected in the dialyzed-out solution during the first dialysis operation (curve c) and it disappeared in the dialyzed-out solution during the last operation (curve d). These results indicated that the dialysis operation was feasible and effective in removing all free luminol and AP^{2-} molecules from the colloids, while retaining the dispersity and stability of the AuNPs. Subsequently, a further salt-out operation was executed on the dialyzed colloid and observable coagulation appeared after the addition of salts. The dual-peak absorption of luminol appeared again in the supernatant after centrifugation (Figure 3, curve e). The precipitates were collected and redissolved in Na_2CO_3 solution. The TEM image (Figure 2F) of this redispersed colloid indicated that the diameter of the nanoparticles increased and the monodispersity became worse during the salting-out process, compared with the original (Figure 2C). The maximal surface plasmon absorption wavelength increased from 534.5 nm (Figure 3, curve b) to 552.0 nm (curve f) and the peak became wide, which further confirmed the results from the TEM images. The information obtained from both TEM images and UV/visible spectra demonstrated that the protective molecules were partially dissociated from the surface of the AuNPs and the repulsive interaction became weak during the salt-out process, which is the reason why the luminol molecules could be detected again in the supernatant. On the other hand, these results also provided evidence for the existence of luminol on the surface of AuNPs.

X-ray photoelectron spectroscopy: Figure 4 shows the Au 4f, C 1s, and N 1s X-ray photoelectron spectra of pure luminol and the as-prepared luminol-reduced AuNPs after further treatments. All binding energies (BEs) were calibrated with respect to the C 1s BE at 284.6 eV.[34] The spin–orbit splitting of doublet components for Au $4f_{7/2}$ and Au $4f_{5/2}$ were measured to be 3.7 eV (Figure 4A), which is in good agreement with previous results.[35] This finding is supporting evidence for the presence of Au^0 in as-prepared AuNPs. As can be seen from Figure 4B, the C 1s spectrum of pure luminol was curve-fitted into three components at 284.6, 286.0, and 287.4 eV. The maximal peak centered at 284.6 eV was attributed to the aromatic carbon atoms in the luminol molecules. The component at 286.0 eV was associated with the carbon atom in the aromatic ring linked to the amine group (C-NH_2).[36] The component at 287.4 eV was due to the carbon atom in the amide group (−CO−NH−).[37] The C 1s spectrum of luminol-reduced AuNPs is shown in Figure 4C. Compared with the C 1s spectrum of pure luminol, a new component centered at 288.6 eV appeared as well as the three components similar to those in the luminol C 1s spectrum, which was attributed to the carbon atom in the carboxylic group (−COO−) of AP^{2-}.[37] This result strongly supported the notion that luminol and AP^{2-} coexisted on the surface of the AuNPs.

Furthermore, the relative area of the 287.4 eV component (−CO−NH−) was much smaller than that of the 288.6 eV component (−COO−). As the former component was particular to luminol and the latter one to AP^{2-}, it is believed that AP^{2-} was the main capping compound on the surface. This phenomenon was probably caused by a difference in their molecular structures. The electronic density of nitrogen in the amine group of luminol is much lower than that of AP^{2-}, as there is an additional conjugated π bond in the amide ring structure. Therefore, the affinity between luminol and gold atoms should be much weaker than that between AP^{2-} and gold atoms, according to the covalent bond model for the interaction between amines and AuNPs,[19,22,23] and consequently the content of luminol on the surface was relatively low.

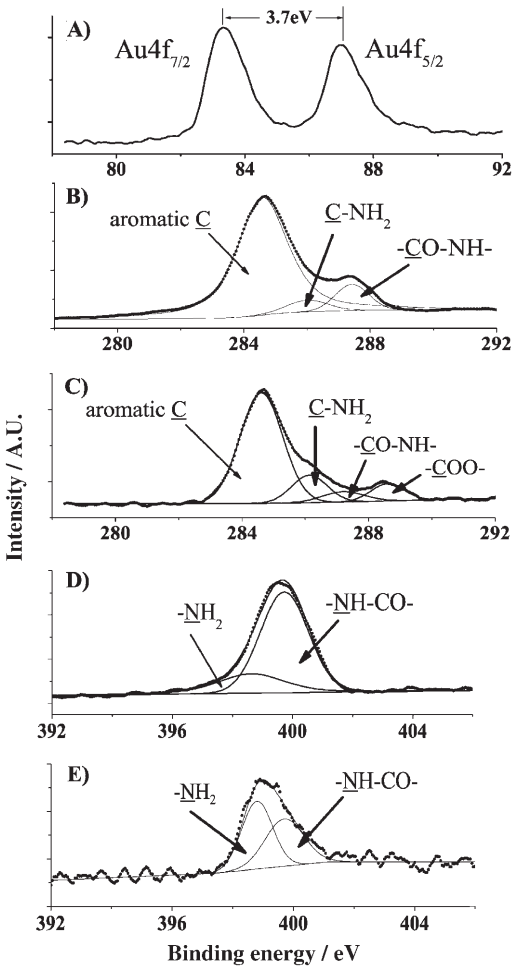

Figure 4. X-ray photoelectron spectra of B) C 1s and D) N 1s of pure luminol and A) Au 4f, C) C 1s, and E) N 1s of luminol-reduced AuNPs.

The analysis of the N 1s spectra was consistent with the above discussion. The N 1s spectra of both luminol and AuNPs (Figure 4D and E, respectively) were curve-fitted into two components at 398.8 and 399.7 eV, attributed to the nitrogen atoms in the amine group (−NH$_2$) and amide group (−CO−NH−), respectively.[37,38] A large decrease in the relative content of the 399.7 eV component (−CO−NH−) demonstrated the relatively low content of luminol on the surface of the nanoparticles, as this component was particular

to luminol and the 398.8 eV component ($-NH_2$) was mutual for both luminol and AP^{2-}. Notably, the N 1s spectrum of luminol-reduced AuNPs also confirmed the absence of the protonated state ($-NH_3^+$) reported to be at approximately 402.3 eV.[39] Consequently, the electrostatic interaction between the protonated amino group and negatively charged AuNPs did not exist, which was reported to occur in the other fatty-amine-protected AuNPs in aqueous solution.[19] In addition, the Au–N covalent interaction was the only force between the gold core and the luminol/AP^{2-} capping molecules.[22,23] This interaction might be caused by the lower electronic density of the aromatic amino group compared to the aliphatic one.

Thermogravimetric analysis: Figure 5 shows the TGA and corresponding differential thermogravimetry (DTG) curves of pure luminol and luminol-reduced AuNPs (Figure 5A

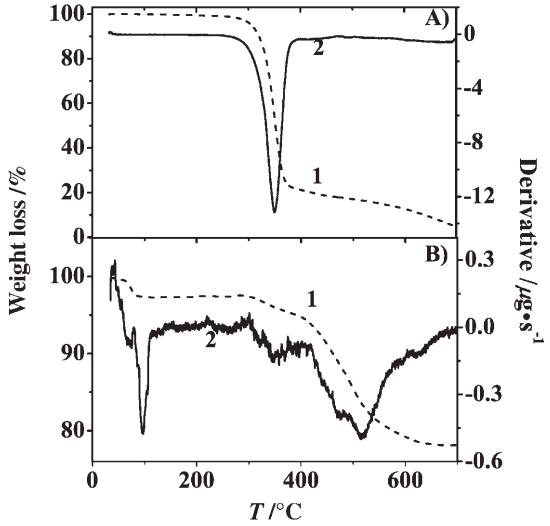

Figure 5. TGA (1) and DTG (2) curves of A) pure luminol and B) luminol-reduced AuNPs.

andB, respectively). Curve 1 is the TGA curve (left axis) and curve 2 is the corresponding DTG curve (right axis) in both cases. For pure luminol, a nearly total weight loss occurred during heating to 700 °C, which started at 290 and ended at 390 °C, with the maximal rate of weight loss at approximately 350 °C. For luminol-reduced AuNPs, a similar weight-loss peak was also observed at approximately 350 °C with 2.5 % weight loss from 280 to 380 °C (Figure 5B). The results support the proposal that luminol exists on the surface of AuNPs. The weight loss around 70 °C in Figure 5B was attributed to the moisture content due to the preparative method. The maximal weight loss of luminol-reduced AuNPs occurred at approximately 520 °C with 17 % weight loss at 390–650 °C, which was satisfactorily consistent with the previously reported TGA data of fatty-amine-capped AuNPs.[19] In that work, two prominent weight-loss peaks were observed at 260 and 500 °C for the Au–octadecylamine complex, and at 255 and 520 °C for the Au–laurylamine complex. The lower characteristic temperature was attributed to the loss of the electrostatically bound fatty amine component and the higher one was due to the loss of the weak covalent interaction between them. The absence of weight loss at approximately 250 °C and the presence of weight loss at approximately 520 °C in the TGA data of luminol-reduced AuNPs further confirmed the results from the N 1s X-ray photoelectron spectrum, which indicated that there was only a covalent interaction and no electrostatic interaction in these luminol-reduced AuNPs. Furthermore, it was concluded that AP^{2-} was the main composition on the surface of the AuNPs rather than luminol, from a comparison of weight-loss peaks at approximately 350 and 520 °C, which was also in agreement with the results of XPS.

FTIR spectroscopy: The IR spectrum of as-prepared AuNPs (Figure 6) further confirmed the surface composition dis-

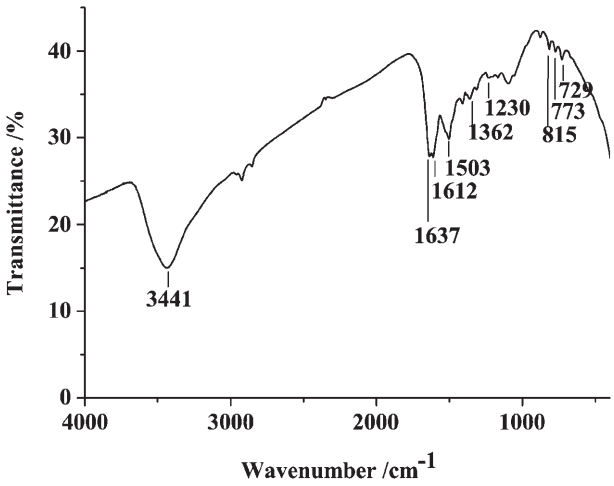

Figure 6. FTIR spectrum of luminol-reduced AuNPs.

cussed above. The existence of luminol can be supported by several characteristic IR absorption bands, including three amide bands[40–42] at 1637, (amide I, the C=O stretching vibration of the amide group), 1530 (amide II, the N–H bending and stretching modes, which can only be observed as the shoulder peak around 1503 cm^{-1}), and 1315 cm^{-1} (amide III, ν_{C-N}, the in-phase combination of N–H in-plane bending and C–N stretching vibrations), the benzene ring absorption bands below 1000 cm^{-1}, and the aromatic ring C=C stretching vibration bands[40] at 1612 and 1503 cm^{-1}. The absorption band at 1411 cm^{-1} (ν_s COO^-) was attributed to the symmetric carboxylate stretch.[42–44] The corresponding antisymmetric carboxylate stretch at approximately 1570 cm^{-1} (ν_{as} COO^-)[42–44] might be overlapped in the strong absorption band at 1612 cm^{-1}, and thus can only be observed as a shoulder peak around this position. These two bands indicated that the AP^{2-} molecules existed as carboxyl salts on

the particle surface. These results were in good agreement with the coadsorption model of luminol and AP^{2-} on the particle surface. Furthermore, the typical doublets of the amino group in the luminol standard IR spectrum[45] around 3400 cm^{-1} (ν_{N-H}) disappeared and only one broad band appeared in the range of 3000–3700 cm^{-1}, which was a reflection of the weak covalent interaction between the amino group and the AuNPs.

Immobilization of luminol on a gold electrode: The as-prepared 20 nm luminol-reduced AuNPs were assembled by cysteine (cys) on the surface of a gold electrode to obtain an AuNP/cys/Au electrode, according to the steps described in the Experimental Section, in order to study the ECL of luminol capped on the surface of AuNPs. From the results above, most of the molecules covering the surface of the AuNPs were AP^{2-}, and only a small number were luminol. To obtain strong ECL, the AuNP/cys/Au electrode was immersed in the luminol solution so that AP^{2-} on the surface of the AuNPs could be replaced by luminol through a place-exchange mechanism,[19] and thus a luminol-capped AuNP/cys/Au (luminol-AuNP/cys/Au) electrode was obtained. The modified electrodes were characterized by CV, EIS, and SEM. Figure 7 shows SEM images of a luminol-AuNP/cys/Au electrode and a bulk Au electrode. The images reveal that AuNPs were distributed evenly on the surface of the electrode. Furthermore, Figure 8A shows the results of EIS on bare gold, cys/Au, AuNP/cys/Au, and luminol-AuNP/cys/Au electrodes in a phosphate buffer solution (PBS; 0.1 mol L^{-1}, pH 7.0) containing $[Fe(CN)_6]^{3-}$ and $[Fe(CN)_6]^{4-}$ (both 1×10^{-3} mol L^{-1}). The impedance spectra consisted of a semicircle at high-ac modulation frequency and a line at low-ac modulation frequency, thus demonstrating that the electrode process was controlled by electron transfer at high frequency and by diffusion at low frequency.[46,47] The smaller the semicircle, the smaller the electron-transfer resistance. The magnitude of the electron-transfer resistance increased in the following order: Au < cys/Au < AuNP/cys/Au.

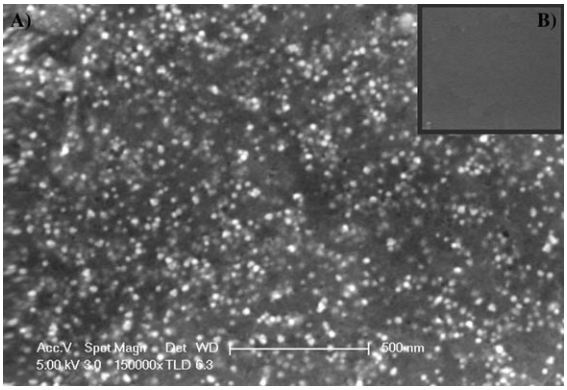

Figure 7. SEM images of A) an as-prepared luminol-AuNP/cys-modified gold electrode and B) a bare gold electrode.

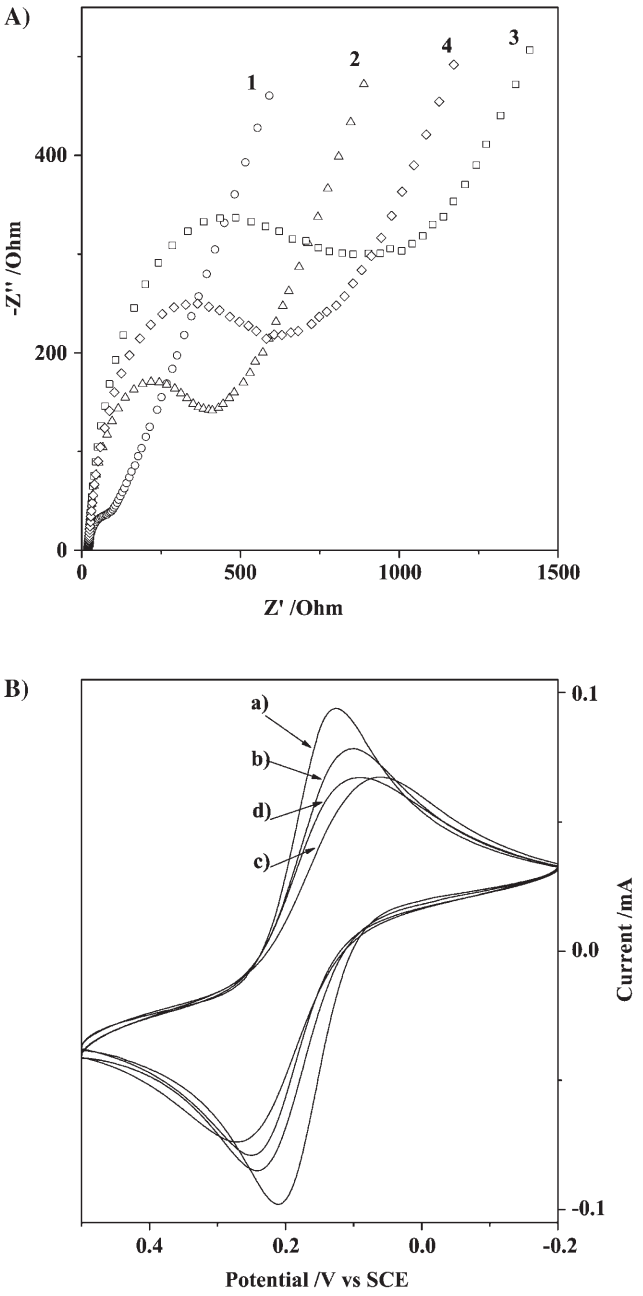

Figure 8. A) Nyquist diagram ($-Z''$ versus Z') of EIS data and B) CV curves of $[Fe(CN)_6]^{3-}/[Fe(CN)_6]^{4-}$ (1×10^{-3} mol L^{-1}) in PBS solution (0.1 mol L^{-1}, pH 7.0) on the modified electrodes. Au electrode: curve 1; cys/Au electrode: curve 2; AuNP/cys/Au electrode: curve 3; luminol-AuNP/cys/Au electrode: curve 4.

When AP^{2-} covering the surface of the AuNP/cys/Au electrode was replaced by luminol, the electron-transfer resistance of the luminol-AuNP/cys/Au electrode decreased. $[Fe(CN)_6]^{3-/4-}$ is a negatively charged redox probe for electron transfer. The negative charge of the electrode surface interface layer would lead to a barrier for the redox process, and therefore increase the electron-transfer resistance.[48] The surface electrical property of the AuNP colloid at pH 7.0 can be deduced from the pK_a values of both luminol

and AP^{2-}. It was reported that the pK_a values are 6.7 (pK_a1) and 15.0 (pK_a2) for luminol[49] and 3.0 (pK_a1) and 5.7 (pK_a2) for AP^{2-}.[50] Therefore, luminol molecules and the monoanionic form coexisted on the surface, whereas the AP^{2-} molecules are almost completely dianionic in PBS at pH 7.0. After immersion in a luminol solution, the negative charge on the surface of the AuNPs declined through the place-exchange mechanism of capping molecules from dianionic AP^{2-} to monoanionic/molecular luminol. Consequently, an increase in electron-transfer resistance on the AuNP/cys/Au electrode was attributed to the negatively charged AuNPs, and a decrease in electron-transfer resistance on the luminol-AuNP/cys/Au electrode was associated with the decrease of the negative interface charge.

The peak current and the peak-to-peak potential distance (DE_p) of the CV curves also revealed information about the electron-transfer process. Figure 8B shows the corresponding CV curves on bare gold (curve a), cys/Au (curve b), AuNP/cys/Au (curve c), and luminol-AuNP/cys/Au (curve d) electrodes, in the same working solution mentioned above. Both peak currents and the DE_p values indicated that the sequence of electron-transfer resistance was Au < cys/Au < luminol-AuNP/cys/Au < AuNP/cys/Au electrodes, which was completely consistent with the EIS results.

ECL of luminol capped on the surface of the AuNP/cys/Au electrode and its analytical application: Luminol molecules were successfully immobilized on the surface of the electrode. It was found that the resulting electrode could directly generate ECL in alkaline solution without any addition of ECL reagent, and excited-state AP^{2-} was identified as the ECL luminophor by the Gaussian-fitted ECL spectrum centered at 425 nm (see Figure 9). The ECL intensity of the resulting electrode increased with the concentration of the H_2O_2 solution. This property offers the possibility that the as-prepared modified electrode could be used as an ECL sensor for the detection of H_2O_2.

An electropulse signal double-step potential was used to initiate the ECL of luminol, as shown in the inset of Figure 10. When a double-step potential was applied to the electrode, a pulse ECL signal was obtained. Moreover, the pulse ECL intensity decreased rapidly at the first stage and then reached a stable value in five to ten periods in every experiment. The average intensity of three pulse ECL signals in the stable area was used as an analytical signal for the detection of H_2O_2 (Figure 10). To

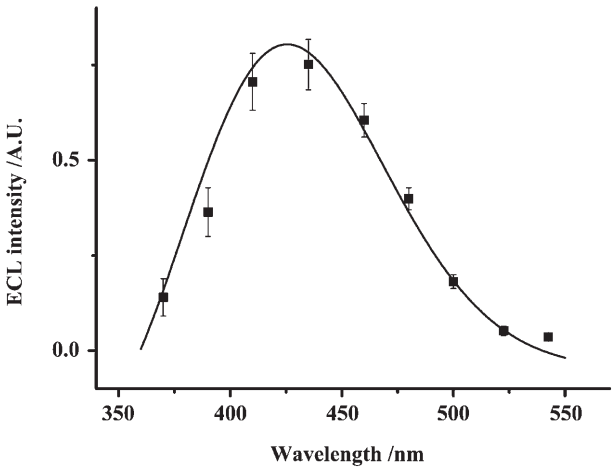

Figure 9. ECL spectrum of an as-prepared luminol-AuNP-modified gold electrode in carbonate buffer solution.

obtain the maximal ECL intensity, the effects of pH, pulse period, pulse potential, and initial potential on the ECL intensity were investigated. It is well known that the luminol ECL depends greatly on the pH of the solution. The effect of pH was examined in the range of 9.3–10.7 in carbonate buffer solution (CBS, 0.1 mol L^{-1}), and a maximal ECL intensity was obtained at pH 10.2 (see Figure 11A). The effect of pulse period on the ECL intensity was investigated in the range of 10–60 s in CBS solution (0.1 mol L^{-1}) at pH 10.2 (see Figure 11B). The ECL signal showed a positive correlation with the pulse period. This phenomenon was attributed to the more effective diffusion of H_2O_2 in the longer pulse period. To make a compromise between higher ECL intensity and shorter analytical time, a pulse period of 30 s was chosen in the following experiments. The pulse potential

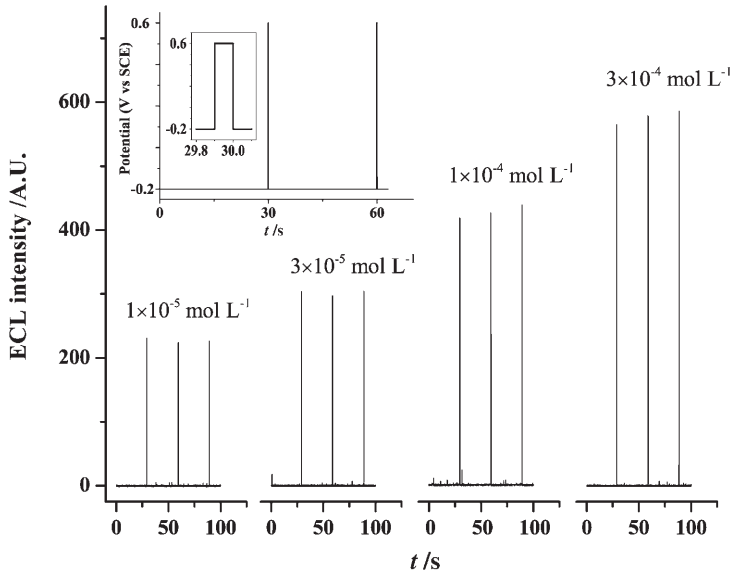

Figure 10. ECL profiles in different concentrations of H_2O_2 solution under three continuous-pulse periods. The inset shows the time dependence of the potential applied on the working electrode. Experimental parameters: initial potential = −0.2 V, pulse potential = 0.6 V, pulse period = 30 s, pulse t = 0.1 s.

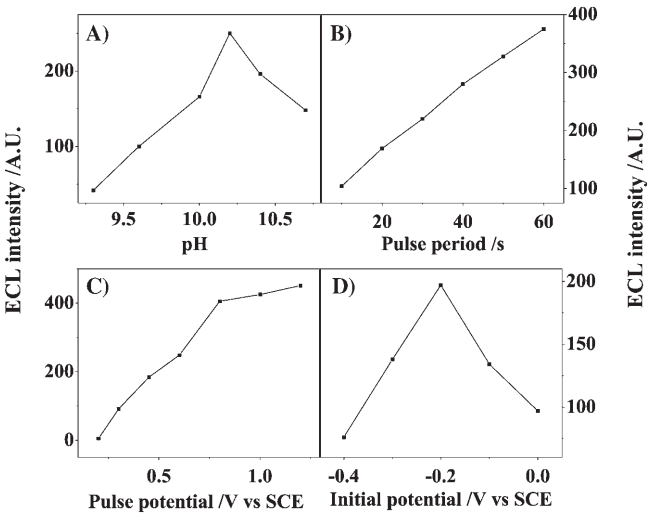

Figure 11. Effects of A) pH, B) pulse period, C) pulse potential, and D) initial potential on ECL intensity.

over the range 0.2–1.2 V (versus SCE) was studied (see Figure 11C). As the electrooxidation of luminol was much faster at higher electrode potentials, a positive correlation between pulse potential and ECL intensity was also observed. However, if a high potential above 0.8 V was selected, the electrooxidation of gold atoms on the surface of the electrode and the Au–S bond between the cysteine molecules and the gold electrode would cause great damage to the stability and reproducibility of the modified electrode. Thus, a pulse potential of 0.6 V was chosen. The effect of initial potential on the ECL intensity was also tested in the range from 0 to −0.4 V (Figure 11D), and maximal ECL intensity was achieved at the initial potential of −0.2 V. Therefore, this initial potential was used in the following experiments.

Under the optimal conditions described above, the change of ECL intensity with the concentration of H_2O_2 is shown in Figure 10. The logarithm of ECL intensity increased linearly with the logarithm of H_2O_2 concentration in the range of 3×10^{-7}–1×10^{-3} mol L^{-1}, and the regression equation was $\log I = 3.7303 + 0.2716 \log C$ ($r = 0.9994$, $n = 8$). The detection limit for H_2O_2 was 1×10^{-7} mol L^{-1} (signal-to-noise ratio $S/N = 3$). The relative standard deviation (RSD) was 6.14% for the determination of 1×10^{-5} mol L^{-1} H_2O_2 ($n = 7$). The results demonstrated that the ECL sensor is applicable to the detection of H_2O_2.

When the proposed sensor is used for H_2O_2 determination, the immobilized luminol on the electrode surface might be consumed during the measurements. Accordingly, the stability of the ECL sensor was examined during consecutive measurements and long-term storage. The ECL intensities obtained by using 650 consecutive pulses in a 1×10^{-3} mol L^{-1} H_2O_2 solution were tested. The results indicated that the ECL intensity of the as-prepared sensor still maintained 80% of its initial value after more than 600 pulse periods in about 5 h, even in such a high concentration of H_2O_2 solution. Therefore, the consumption of immobilized luminol was acceptable during the consecutive measurements. Besides, the exhausted sensor can be partially self-healed by immersion in a luminol solution through the place-exchange mechanism of capping molecules. The long-term stability of the sensor was also studied. It was found that the ECL intensity of the sensor gradually decreased when it was stored in distilled water or PBS (0.1 mol L^{-1}) at pH 7.0 and underwent three sets of measurements in a 1×10^{-5} mol L^{-1} H_2O_2 solution every day. The intensity decreased by more than 40% in three days when the sensor was stored in distilled water, which was better than that in PBS. This decrease might be partially due to the desorption of luminol AuNPs from the electrode, as the luminol AuNPs were linked to the electrode by electrostatic interactions. The improvement of the long-term stability of the ECL sensor is under further investigation.

Conclusion

This work has demonstrated that AuNPs with diameters of 14–35 nm could be synthesized by the direct reaction between $HAuCl_4$ and luminol in aqueous solution, and that the diameter of the nanoparticles increased with decreasing amounts of reductant luminol. UV/Vis spectroscopy, XPS, TGA, and FTIR spectroscopy showed that luminol and its oxidation product AP^{2-} coadsorbed on the surface of AuNPs through the weak covalent interaction between gold and nitrogen atoms in the amino groups, and that AP^{2-} was the main capping compound on the surface. Subsequently, a luminol-capped AuNP-modified electrode was fabricated by the immobilization of AuNPs on a gold electrode by virtue of cysteine molecules and immersion in luminol solution. It was found that luminol capped on the surface of the AuNP-modified electrode could directly generate ECL under a double-step potential. A reagent-free ECL sensor for the detection of H_2O_2 was developed based on the modified electrode. The sensor was applicable to the detection of H_2O_2 in the range of 3×10^{-7}–1×10^{-3} mol L^{-1} with a detection limit of 1×10^{-7} mol L^{-1} ($S/N = 3$).

This work shows for the first time that luminol could be immobilized as a capping reagent of AuNPs assembled on an electrode for developing a H_2O_2 ECL sensor. By virtue of the coimmobilization technique with enzymes, ECL sensors for the detection of biologically important compounds are under investigation based on the immobilization of luminol. The response of H_2O_2 as a model compound to the modified electrode was examined. The response of compounds other than H_2O_2 to the modified electrode is also being explored to extend the applications of the luminol-immobilized electrode.

Experimental Section

Chemical and solutions: A stock solution of luminol (0.01 mol L^{-1}) was prepared by dissolving luminol (Sigma) in NaOH solution (0.1 mol L^{-1})

without further purification. Working solutions of luminol were prepared by diluting the stock solution. $HAuCl_4{\cdot}4H_2O$ was obtained from Shanghai Reagent (Shanghai, China). An $HAuCl_4$ stock solution ($1.0\,g\,L^{-1}$) was prepared by dissolving $HAuCl_4$ (1 g) in redistilled water (1 L) and stored at 4 °C. Working solutions of H_2O_2 were prepared fresh daily from 30% (v/v) H_2O_2 (Xinke Electrochemical Reagent Factory, Bengbu, China). All other reagents were of analytical grade, and redistilled water was used throughout.

Synthesis and characterization of AuNPs: All glassware used in the following procedures was cleaned in a bath of freshly prepared HNO_3/HCl (3:1, v/v), rinsed thoroughly in redistilled water, and dried prior to use. Gold colloids with various diameters were prepared by the reduction of $HAuCl_4$ with luminol, which was similar to the classical citrate reduction method.[51] A 100 mL portion of $HAuCl_4$ solution (0.01%, w/w) was heated to boiling point. While stirring vigorously, various amounts of luminol solution ($0.01\,mol\,L^{-1}$) were added rapidly. Volumes of 1.45, 1.50, 1.55, 1.60, and 1.80 mL were selected for synthesizing AuNPs with different diameters. The solution was maintained at boiling point for 30 min, during which time a color change from yellow to black to purple was observed before a wine-red or purple color was reached. The heating source was removed, and the colloid was kept at room temperature for another 20 min and then stored at 4 °C. Note that the pH of the added luminol solution played a very important role in the preparation of the gold colloids. The diameters of as-prepared AuNPs were found to be very different when a luminol stock solution with 0.1 or $0.05\,mol\,L^{-1}$ NaOH was used. If other conditions were controlled such that they were identical, the synthetic reaction was much faster and formed AuNPs of larger diameters in the luminol stock solution at lower pH.

Gold colloids prepared with 1.55 mL luminol were used for the characterization. As-synthesized colloidal solutions were characterized by TEM (Hitachi H-800, Japan) and UV/Vis spectroscopy (Shimadzu UV-2401 PC spectrophotometer, Japan). A salt-out procedure was introduced to exclude the effect of excess luminol and other coexisting free molecules in the colloids on the characterization of the surface state of AuNPs. In a typical salt-out procedure, a suitable amount of NaCl (KBr for FTIR experiments) was added to the gold colloids and the resulting precipitates were washed twice with redistilled water through a repeated ultrasonic dispersion–centrifugation process to remove inorganic or organic impurities completely. Finally, the AuNPs were dried under vacuum at room temperature. The obtained dry powders of AuNPs were used to acquire XPS, FTIR, and TGA data. XPS was performed on an ESCALAB MK II electron spectrograph (VG Scientific, UK). The FTIR experiments were carried out on a Bruker Vector-22 FTIR spectrometer (Bruker Instruments, Billerica, MA) in a KBr pellet, scanning from 4000 to $400\,cm^{-1}$ at room temperature. The TGA data were acquired on a Shimadzu TA-50 thermal analyzer (Shimadzu, Japan) at a heating rate of $5\,°C\,min^{-1}$ from room temperature to 700 °C in a nitrogen atmosphere.

A dialysis operation was used to separate excess luminol from the colloids instead of the salt-out strategy, to avoid the aggregation of AuNPs during the salt-out process. A homemade semipermeable membrane was used, which was prepared by the volatilization of collodion. Redistilled water was refreshed about six to ten times under stirring until no absorption was observed in the UV/Vis spectrum of the dialyzed-out solution. A typical dialysis operation needed about 24 h.

Preparation and characterization of AuNP-modified electrode: Scheme 1 shows the procedures for preparing the luminol-AuNP/cys-modified gold electrode proposed in this work. The bare gold electrode was polished to a mirrorlike surface with chamois leather, rinsed with redistilled water, and then dried with filter paper. The electrode was then cleaned by cycling between 0 and 1.5 V versus SCE in H_2SO_4 ($0.5\,mol\,L^{-1}$) at a scan rate of $100\,mV\,s^{-1}$ until reproducible cyclic voltammograms were obtained. This freshly pretreated bare Au electrode was immersed in L-cysteine solution ($0.1\,mol\,L^{-1}$) for 4 h at room temperature in darkness to allow the self-assembling of cysteine on the surface of the electrode. The resulting monolayer-modified electrode was rinsed thoroughly with redistilled water to remove the physically adsorbed cysteine. Then the cys/Au electrode was dipped into the gold colloid solution for 18 h at 4 °C. Gold colloid prepared with 1.60 mL of luminol was selected for the modification procedures. Subsequently, the AuNP self-assembled electrode (AuNP/cys/Au electrode) was dipped into luminol solution ($1\times10^{-3}\,mol\,L^{-1}$) for another 12 h at 4 °C. Finally, the as-prepared modified electrode (luminol-AuNP/cys/Au electrode) was dipped into redistilled water for conservation at 4 °C.

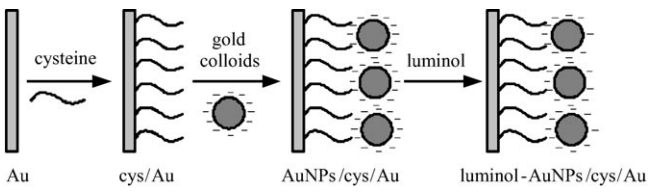

Scheme 1. Preparation procedure of the luminol-AuNP/cys/Au electrode.

CV, EIS, and SEM were used to monitor the modification procedures. SEM was performed on a JEOL JSM-6700F microscope (JEOL, Japan). Both CV and EIS experiments were carried out on a CHI760B electrochemical workstation (Chenhua, China). PBS ($0.1\,mol\,L^{-1}$, pH 7.0) containing $[Fe(CN)_6]^{3-}+[Fe(CN)_6]^{4-}$ (both $1\times10^{-3}\,mol\,L^{-1}$) was used as working solution. The EIS results were recorded in the frequency range of 0.1 to 10 kHz at the formal potential of the corresponding redox couple and with a 5 mV amplitude of the alternating voltage.

ECL measurements: ECL measurements were performed with a homemade ECL/electrochemical cell system, including a model CHI760B electrochemical workstation (Chenhua, China), an H-type electrochemical cell (self-designed), a model CR-105 photomultiplier tube (PMT) (Beijing, China), a model RFL-1 luminometer (Xi'an, China), and a computer, as described previously.[52,53] A luminol-AuNP/cys-modified gold electrode served as the working electrode, a platinum wire as the counter electrode, and a silver wire as the quasi-reference electrode (AgQRE). Although the potential of the AgQRE was essentially stable during an experiment, the measurements of $\Delta E = E_{Ag/Ag+} - E_{SCE}$ in different solutions were taken for potential calibrations. A H_2O_2 solution containing CBS ($0.1\,mol\,L^{-1}$) was used as working solution for the determination of H_2O_2. During measurements, a 2.0 mL portion of the working solution and the blank solution without H_2O_2 were added to the working compartment and the auxiliary compartment of the ECL cell, respectively. When a double-step potential was applied to the working electrode, an ECL signal was generated and recorded.

The ECL spectrum was measured by inserting filters at wavelengths of 360, 380, 400, 420, 450, 470, 490, 510, 535, and 550 nm (light cannot pass at wavelengths lower than these) under pulse conditions, as described previously.[25] I_λ was calculated as $I_{(\lambda1+\lambda2)/2} = (I_{\lambda2} - I_{\lambda1})/(\lambda_2 - \lambda_1)$, for example, $I_{390} = (I_{400} - I_{380})/(400-380)$, $I_{435} = (I_{450} - I_{420})/(450-420)$, etc. The curve of I_λ versus λ was consistent with the ECL emission spectrum.

Acknowledgements

Support of this research by the National Natural Science Foundation of China (grant nos. 20375037 and 20625517) and the Overseas Outstanding Young Scientist Program of the Chinese Academy of Sciences is gratefully acknowledged. The authors also wish to thank Dr. P. Buhlmann at the University of Minnesota for the helpful discussion on the different affinities of luminol and AP^{2-} to AuNPs, and constructive suggestions on the EIS experiments.

[1] A. W. Knight, *TrAC Trends Anal. Chem.* **1999**, *18*, 47–62.
[2] K. A. Fahnrich, M. Pravda, G. G. Guilbault, *Talanta* **2001**, *54*, 531–559.
[3] M. M. Richter, *Chem. Rev.* **2004**, *104*, 3003–3036.
[4] X. B. Yin, E. K. Wang, *Anal. Chim. Acta* **2005**, *533*, 113–120.
[5] F. Li, Y. Q. Pang, X. Q. Lin, H. Cui, *Talanta* **2003**, *59*, 627–636.

[6] R. J. Forster, C. F. Hogan, *Anal. Chem.* **2000**, *72*, 5576–5582.
[7] H. N. Choi, S. H. Cho, W. Y. Lee, *Anal. Chem.* **2003**, *75*, 4250–4256.
[8] Z. H. Guo, Y. Shen, M. K. Wang, F. Zhao, S. J. Dong, *Anal. Chem.* **2004**, *76*, 184–191.
[9] Z. H. Guo, S. J. Dong, *Anal. Chem.* **2004**, *76*, 2683–2688.
[10] X. P. Sun, Y. Du, S. J. Dong, E. K. Wang, *Anal. Chem.* **2005**, *77*, 8166–8169.
[11] L. H. Zhang, Z. A. Xu, X. P. Sun, S. J. Dong, *Biosens. Bioelectron.* **2006**, *22*, 1097–1100.
[12] C. S. Ouyang, C. M. Wang, *J. Electrochem. Soc.* **1998**, *145*, 2654–2659.
[13] L. L. Zhang, X. W. Zheng, *Anal. Chim. Acta* **2006**, *570*, 207–213.
[14] K. J. Qian, L. Zhang, M. L. Yang, P. G. He, Y. Z. Fang, *Chin. J. Chem.* **2004**, *22*, 702–707.
[15] J. Wang, *Small* **2005**, *1*, 1036–1043.
[16] L. Murphy, *Curr. Opin. Chem. Biol.* **2006**, *10*, 177–184.
[17] M. Aslam, L. Fu, M. Su, K. Vijayamohanan, V. P. Dravid, *J. Mater. Chem.* **2004**, *14*, 1795–1797.
[18] J. D. S. Newman, G. J. Blanchard, *Langmuir* **2006**, *22*, 5882–5887.
[19] A. Kumar, S. Mandal, P. R. Selvakannan, R. Pasricha, A. B. Mandale, M. Sastry, *Langmuir* **2003**, *19*, 6277–6282.
[20] Y. Shao, Y. D. Jin, S. J. Dong, *Chem. Commun.* **2004**, 1104–1105.
[21] P. R. Selvakannan, S. Mandal, S. Phadtare, A. Gole, R. Pasricha, S. D. Adyanthaya, M. Sastry, *J. Colloid Interface Sci.* **2004**, *269*, 97–102.
[22] M. Sastry, A. Kumar, P. Mukherjee, *Colloids Surf. A* **2001**, *181*, 255–259.
[23] D. V. Leff, L. Brandt, J. R. Heath, *Langmuir* **1996**, *12*, 4723–4730.
[24] Imdadullah, T. Fujiwara, T. Kumamaru, *Anal. Chem.* **1991**, *63*, 2348–2352.
[25] H. Cui, Y. Xu, Z. F. Zhang, *Anal. Chem.* **2004**, *76*, 4002–4010.
[26] B. X. Li, Z. J. Zhang, L. X. Zhao, *Anal. Chim. Acta* **2001**, *445*, 161–167.
[27] G. J. Zhou, G. Wang, J. J. Xu, H. Y. Chen, *Sens. Actuators B* **2002**, *81*, 334–339.
[28] O. Nozaki, H. Kawamoto, *Anal. Chim. Acta* **2003**, *495*, 233–238.
[29] S. Link, M. A. El-Sayed, *J. Phys. Chem. B* **1999**, *103*, 4212–4217.
[30] K. S. Mayya, V. Patil, M. Sastry, *Langmuir* **1997**, *13*, 3944–3947.
[31] S. Roux, B. Garcia, J. L. Bridot, M. Salome, C. Marquette, L. Lemelle, P. Gillet, L. Blum, P. Perriat, O. Tillement, *Langmuir* **2005**, *21*, 2526–2536.
[32] B. V. Enustun, J. Turkevich, *J. Am. Chem. Soc.* **1963**, *85*, 3317–3328.
[33] A. N. Shipway, M. Lahav, R. Gabai, I. Willner, *Langmuir* **2000**, *16*, 8789–8795.
[34] K. Lee, F. Pan, G. T. Carroll, N. J. Turro, J. T. Koberstein, *Langmuir* **2004**, *20*, 1812–1818.
[35] M. F. Lengke, M. E. Fleet, G. Southam, *Langmuir* **2006**, *22*, 2780–2787.
[36] P. G. Ganesan, A. P. Singh, G. Ramanath, *Appl. Phys. Lett.* **2004**, *85*, 579–581.
[37] S. R. Puniredd, M. P. Srinivasan, *Langmuir* **2006**, *22*, 4092–4099.
[38] F. Cecchet, G. Fioravanti, M. Marcaccio, M. Margotti, L. Mattiello, F. Paolucci, S. Rapino, P. Rudolf, *J. Phys. Chem. B* **2005**, *109*, 18427–18432.
[39] O. Seitz, M. M. Chehimi, E. Cabet-Deliry, S. Truong, N. Felidj, C. Perruchot, S. J. Greaves, J. F. Watts, *Colloids Surf. A* **2003**, *218*, 225–239.
[40] K. Nakanishi, P. H. Solomon, *Infrared Absorption Spectroscopy*, 2nd ed., Holden-Day, San Francisco, **1977**, pp. 19 and 42.
[41] S. H. Chen, H. Yao, K. Kimura, *Langmuir* **2001**, *17*, 733–739.
[42] K. S. Mayya, F. Caruso, *Langmuir* **2003**, *19*, 6987–6993.
[43] A. D. Roddick-Lanzilotta, P. A. Connor, A. J. McQuillan, *Langmuir* **1998**, *14*, 6479–6484.
[44] S. H. Chen, K. Kimura, *Langmuir* **1999**, *15*, 1075–1082.
[45] http://www.sigmaaldrich.com/spectra/ftir/FTIR000532.PDF (visited on 13 Dec **2006**).
[46] H. Y. Gu, A. M. Yu, H. Y. Chen, *J. Electroanal. Chem.* **2001**, *516*, 119–126.
[47] B. Fang, X. H. Deng, X. W. Kan, H. S. Tao, W. Z. Zhang, M. G. Li, *Anal. Lett.* **2006**, *39*, 697–707.
[48] V. Pardo-Yissar, E. Katz, O. Lioubashevski, I. Willner, *Langmuir* **2001**, *17*, 1110–1118.
[49] G. Merenyi, J. Lind, X. Shen, T. E. Eriksen, *J. Phys. Chem.* **1990**, *94*, 748–752.
[50] J. Lind, G. Merenyi, T. E. Eriksen, *J. Am. Chem. Soc.* **1983**, *105*, 7655–7661.
[51] G. Frens, *Nature Phys. Sci.* **1973**, *241*, 20–22.
[52] H. Cui, Z. F. Zhang, G. Z. Zou, X. Q. Lin, *J. Electroanal. Chem.* **2004**, *566*, 305–313.
[53] H. Cui, G. Z. Zou, X. Q. Lin, *Anal. Chem.* **2003**, *75*, 324–331.

Received: January 4, 2007
Published online: May 31, 2007

